12

HDL-CR-83-107-6

Bistatic Radar Cross Sections of Chaff

Peyton Z. Peebles, Jr.

June 1983

Prepared by

The University of Florida
Electronic Communications Laboratory
Engineering and Industrial Experiment Station
Gainesville, Florida 32611

Under contract

DAAK21-82-C-0107

U.S. Army Electronics Research and Development Command
Harry Diamond Laboratories
Adelphi, MD 20783

The findings in this report are not to be construed as an official Department of the Army position unless so designated by other authorized documents.

Citation of manufacturers' or trade names does not constitute an official indorsement or approval of the use thereof.

Destroy this report when it is no longer needed. Do not return it to the originator.

UNCLASSIFIED

SECURITY CLASSIFICATION OF THIS PAGE (When Data Entered)

REPORT DOCUMENTATION PAGE		READ INSTRUCTIONS BEFORE COMPLETING FORM
1. REPORT NUMBER HDL-CR-83-107-6	2. GOVT ACCESSION NO. AD-A133962	3. RECIPIENT'S CATALOG NUMBER
4. TITLE (and Subtitle) Bistatic Radar Cross Sections of Chaff		5. TYPE OF REPORT & PERIOD COVERED Contractor Report 6. PERFORMING ORG. REPORT NUMBER
7. AUTHOR(s) Peyton Z. Peebles, Jr. (HDL contact Barry Stann)		8. CONTRACT OR GRANT NUMBER(s) DAAK21-82-C-0107
9. PERFORMING ORGANIZATION NAME AND ADDRESS University of Florida, Electronic Communications Laboratory, Engineering and Industrial Experiment Station, Gainesville, FL 32611		10. PROGRAM ELEMENT, PROJECT, TASK AREA & WORK UNIT NUMBERS Program element: 6.26.16.A HDL Proj: A7773
11. CONTROLLING OFFICE NAME AND ADDRESS U. S. Army Materiel Development and Readiness Command Alexandria, VA 22333		12. REPORT DATE June 1983 13. NUMBER OF PAGES 39
14. MONITORING AGENCY NAME & ADDRESS(if different from Controlling Office) Harry Diamond Laboratories 2800 Powder Mill Road Adelphi, MD 20783		15. SECURITY CLASS. (of this report) UNCLASSIFIED 15a. DECLASSIFICATION/DOWNGRADING SCHEDULE

16. DISTRIBUTION STATEMENT (of this Report)

Approved for public release; distribution unlimited.

17. DISTRIBUTION STATEMENT (of the abstract entered in Block 20, if different from Report)

18. SUPPLEMENTARY NOTES

Work unit title: Fuze Technology
DA Proj: 1L662616AH77, DRCMS Code: 662616.11.H7700

19. KEY WORDS (Continue on reverse side if necessary and identify by block number)

Bistatic scattering	Radar polarizations
Chaff	Polarization matrix
Radar countermeasure	Dipoles
Radar bistatic cross section	Dipole scattering

20. ABSTRACT (Continue on reverse side if necessary and identify by block number)

Bistatic cross sections applicable to scattering from a cloud of randomly positioned and randomly oriented resonant dipoles, or chaff, are found. The chaff cloud can have an arbitrary location relative to an illuminating radar and the radar antenna can have an arbitrarily specified polarization. The receiver can be located arbitrarily in relation to the radar and chaff cloud and can also have arbitrary polarization (different from transmitter antenna). Average cross sections are found for a preferred receiver polarization, and

DD FORM 1 JAN 73 1473 EDITION OF 1 NOV 65 IS OBSOLETE

UNCLASSIFIED

SECURITY CLASSIFICATION OF THIS PAGE (When Data Entered)

the corresponding orthogonal polarization. Results are reduced to simple, easily applied expressions, and several examples are developed to illustrate the ease with which the general results can be applied in practice.

CONTENTS

FIGURES

FIGURES (Cont.)

TABLES

1. INTRODUCTION

Chaff, which is a countermeasure designed to reduce the effectiveness of radar, has also been used in communications systems. Chaff usually consists of a large number of thin, highly conducting wires dispensed in the atmosphere to form a "cloud" of scatterers. Energy scattered by the cloud and received by a radar would ideally be large enough to mask the presence of some target for which the chaff is to protect. The wires may have many forms but typically are cut to a length so that they become resonant dipoles at the radar's frequency. The dipoles also will be effective at harmonics of the radar frequency. For example, dipoles that are tuned to half-wavelength resonance at frequency f_0 will be full-wave dipoles at $2f_0$, three-halves wavelength at $3f_0$, etc. If one dispenses dipoles of several lengths chaff can be made effective over a wide band of frequencies.

Chaff was first used in World War II to confuse German radar, but it remains an important countermeasure to date. Many parameters enter into the overall effectiveness of chaff, such as physical cross sectional area of chaff elements (dipoles), losses in the elements, speed and extent to which clouds form, effects of winds and turbulance on dipole shape, fall speed and attitudes of the elements, weight, volume, clustering (birdnesting) tendencies, and radar cross section. This paper is concerned only with the radar cross section of chaff. For the reader interested in the other parameters, several survey papers are available. [1-5]†

The literature related to scattering from chaff and from chaff elements is voluminous; no effort will be made to give a comprehensive list of references. For a good listing of articles prior to about 1970 the Radar Cross Section Handbook [6] is a good source. Peebles [7] is a bibliography on the subject up to about 1983. We shall, however, cite a few references considered representative of the developments that have evolved and that related most directly to the interests of this paper.

Early efforts to describe chaff effects centered mainly on backscatter cross section (monostatic scattering). Bloch, Hammermesh, and Phillips [8] gave one of the earliest analyses based on a simple, infinitely conducting, wire model of the dipole; backscatter cross section was found for a dipole element having any orientation relative to the incident wave. In addition, the importance of the randomness of dipole positions and orientations was realized and average cross sections were determined. For chaff elements with directions uniformly distributed over the sphere, cross section was found to be $0.158\lambda^2$ per dipole, a value that is representative to date. For dipoles in the wave's polarization plane, but uniformly distributed in angle within the plane, cross section per dipole was found to be $0.289\lambda^2$ [8].

---

† References are quoted by bracketed numbers and are located at the end of the report.

Apparently, using a dipole model similar to Bloch et al. [8], Chu, in unpublished work cited in Van Vleck et al. [9], found the spherically averaged backscatter cross section, denoted by $\bar{\sigma}$, for resonant dipoles. His result can be put in the form

$$\bar{\sigma}/\lambda^2 = \frac{1.178(L/\lambda) - 0.131 + 0.179 \ln(22.368\ L/\lambda)}{[\ln(22.368\ L/\lambda)]^2} \qquad (1)$$

per dipole, where L is the dipole length, λ is wavelength, and L must be a multiple of $\lambda/2$; i.e., $L = M\lambda/2$, $M = 1,2, \ldots$. From equation (1), $\bar{\sigma} = 0.153\lambda^2$, $0.166\lambda^2$, and $0.184\lambda^2$ for half-wave, full-wave, and 1.5-wave dipoles, respectively.

Much effort has been made over the years to refine and extend the models for dipole scattering. One model based on induced EMF was developed [9]; it was called "Method A" and gave nearly the same results as Chu but was also valid for dipole lengths between resonances and nonzero wire cross-sectional area. A second "Method B" [9] produced better agreement with measured data than Method A and was a first-order integral equation solution. Method B was comparable with an independent development of King and Middleton [10]. Another model due to Tai [11] applied to infinitely conducting dipoles and used a variational method. Cassedy and Fainberg [12] extended the model of Tai to include finite dipole conductivity. Harrison and Heinz [13] have considered backscatter for tubular and strip chaff elements as well as solid wires, all for finite conductivity. A model based on the Wiener-Hopf technique introduced by Chen [14] for thin wires applies to longer dipoles and appears to fit experimental data better than some earlier models. More complicated computer models taking into account mutual coupling between dipoles in a cloud are described by Wickliff and Garbacz [15]. Medgyesi-Mitschang and Eftimiu [16] have used Galerkin Expansions to examine backscattering from infinitely conducting tubes. Other characteristics that have been studied that are applicable to backscatter from chaff are statistical properties [17] and spectral properties due to dipole motion [18, 19].

Whereas considerable effort has been made to describe backscattering, less effort has been made in the more general bistatic scattering problem. One of the earliest studies appears to be that of Hessemer [20], where reflections from chaff were used for communications. Useful formulas were derived for average cross sections assuming both spherical and planar random dipole distributions when using a simple thin wire model (similar to Bloch et al. [8]). Mack and Reiffen [21] also used a thin wire model to find average bistatic cross sections and showed how they depend on linear or circular polarization. Some discussion of the effect of losses was also given. Unfortunately, there has been some question as to the correctness of some results in Mack and Reiffen [21] as pointed out by Harrington [22]. We say more about this below. Borison [23] has also obtained some specific average cross sections, but only for linear polarizations. Other studies of bistatic scattering from dipoles [24-29] have used more exact models, but results obtained are either somewhat difficult to apply in practical cases, or do not give explicit equations for cross section useful to applications, or do not show the way in which geometry

and polarizations of transmit and receive antennas affect the scattering. Some of these efforts also did not obtain the averaged cross section of chaff.

Probably the most complete study of chaff to date is due to Dedrick, Hessing, and Johnson [30]. By applying an approach using Stokes parameters they were able to show that four independent quantities are all that are required to determine any chaff cross section. The results in Dedrick et al. [30] applied to any combination of transmit-receive antenna polarizations, but how to compute results for such combinations was not shown. Results that were given were mainly in the form of graphs derived from simulations, and these were for dipole lengths that are not usually of much interest in practice (no specific equations were given for solutions of the four required parameters).

The most recent analyses of bistatic chaff have used the polarization scattering matrix. Heath [31] has used this approach to show the relations between cross sections applicable to circular transmit-receive polarizations and cross sections applicable to linear field components parallel and normal to the plane containing transmitter, scatterer, and receiver. Other work [32] showed the relationship between circular cross sections and cross sections applicable to linear transmit-receive polarizations.

From the preceding discussion one concludes that the complete solution to the problem of bistatic scattering from chaff, even for the simple dipole model has not been developed. It is the purpose of this paper to present such a solution in a form that is readily applied in practice. Specifically, we shall determine explicit equations for the chaff bistatic cross section presented to a receiving antenna having arbitrary (elliptical) polarization, arbitrary location, and viewing the chaff cloud in an arbitrary direction when the cloud is being illuminated by a transmitter having an arbitrarily polarized (different elliptical) antenna. Our results are in a form that is easy to use; several specific examples of practical interest are developed in detail.

2. PROBLEM DEFINITION AND SUMMARY OF RESULTS

2.1 Problem Definition

The overall geometry applicable to bistatic scattering is shown in figure 1. A transmit antenna located at point T radiates an arbitrarily polarized wave toward a cloud of randomly positioned and randomly oriented dipoles represented by point D.† The transmit direction is defined by spherical coordinate angles, θ_1, ϕ_1, defined in the common x,y,z coordinate frame. The dipole cloud is assumed far enough away that the incident wave is planar. Cloud ex-

†Clearly, point D cannot represent the cloud; it is helpful to view D as a point toward which both transmit and receiver antennas are directed and about which dipoles in the cloud are dispersed.

tent is assumed to be small enough in relation to average distance, denoted by r_1, so that the strength of the incident field is approximately the same for all dipoles.

Scattering between dipoles is assumed negligible, and dipoles are presumed sufficiently dispersed that mutual coupling is of no concern. Study has shown [29] that dipoles spaced at least two wavelengths apart in any direction produce almost no mutual coupling; average spacings down to 0.4λ, λ denoting wavelength, can produce up to a 3-dB loss in bistatic cross section. Dipoles are assumed to be infinitely conducting wires with a length that produces resonance at the transmitter frequency; thus, we shall assume the simple wire model. In many practical cases dipole size and material are such that dipole losses are negligible [33].

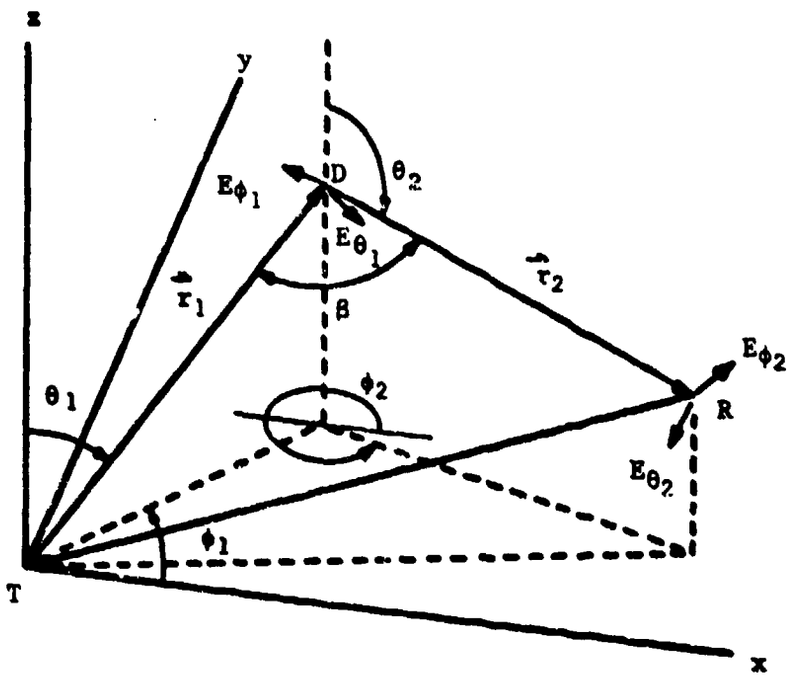

Figure 1. Overall geometry of bistatic scattering.

As illustrated in figure 1, a typical dipole scatters some energy in the direction of a receiver, at point R, defined by spherical angles θ_2, ϕ_2. The receiving antenna is assumed far enough away from all dipoles in the cloud being viewed by the receiver antenna so that all dipole-receiver path distances approximately equal the average distance, denoted by r_2. The receiver is arbitrarily located, and the angle between its line of sight (RD) and the radar's line of sight (TD) is called the bistatic scattering angle, denoted by β.

Both transmit and receive antennas are presumed to be arbitrary; that is, they are elliptically polarized. By employing the usual complex envelope representation of fields, one can define the transmitted (or received) field polarization by a complex quantity Q (Q_T for transmitter; Q_R for receiver) that equals the complex field in the ϕ direction (ϕ_1 for transmitter; ϕ_2 for re-

ceiver) divided by the complex field in the θ direction (θ_1 for transmitter; θ_2 for receiver). Appendix A details ways of selecting Q_T and Q_R for specific systems. The electric field of the wave incident on the dipole cloud is denoted by $\vec{E}_1$; it has components in directions θ_1 and ϕ_1, and its polarization is determined by Q_T. The electric field vector, denoted by $\vec{E}_2$, of the wave arriving at the receiver can be decomposed into the sum of (1) an electric field vector, denoted by $\vec{E}_{R_1}$, of an elliptically polarized wave having the receive antenna's polarization, defined by Q_R, and (2) a second wave's electric field vector, denoted by $\vec{E}_{R_2}$, having the orthogonal polarization also defined by Q_R.

With the above definitions we define bistatic cross section, denoted by σ, based on the power arriving at the receiver in the receiver's preferred polarization according to

$$\sigma = \lim_{r_2 \to \infty} 4\pi r_2^2 \frac{|\vec{E}_{R_1}|^2}{|\vec{E}_1|^2} \sim 4\pi r_2^2 |\vec{E}_{R_1}|^2 / |\vec{E}_1|^2 \quad . \tag{2}$$

Cross section, denoted by σ_x, can also be defined for power arriving at the receiver in the orthogonal polarization by

$$\sigma_x = \lim_{r_2 \to \infty} 4\pi r_2^2 \frac{|\vec{E}_{R_2}|^2}{|\vec{E}_1|^2} \approx 4\pi r_2^2 |\vec{E}_{R_2}|^2 / |\vec{E}_1|^2 \quad . \tag{3}$$

The approximations in equations (2) and (3) are true because we have assumed r_2 relatively large. These cross sections depend on the exact dipole positions and orientations. A reasonable approach to reducing the complexity of equations (2) and (3) is to take advantage of the random nature of positions and orientations by treating these quantities as random variables and averaging to get average cross sections, denoted by $\bar{\sigma}$ and $\bar{\sigma}_x$. By using $E[\cdot]$ to denote the statistical average we have

$$\bar{\sigma} = 4\pi r_2^2 E\left[|\vec{E}_{R_1}|^2\right] / |\vec{E}_1|^2 \quad , \tag{4}$$

$$\bar{\sigma}_x = 4\pi r_2^2 E\left[|\vec{E}_{R_2}|^2\right] / |\vec{E}_1|^2 \quad . \tag{5}$$

2.2 Summary of Results

In following sections we show that

$$\bar{\sigma} = \frac{N}{(1 + |Q_T|^2)(1 + |Q_R|^2)} \left\{ \left(\bar{\sigma}_{\perp \text{to} \perp} |W_1|^2 + \bar{\sigma}_{\perp \text{to} \parallel} |W_2|^2 \right) |X_1|^2 \right.$$
$$+ \left(\bar{\sigma}_{\perp \text{to} \parallel} |W_1|^2 + \bar{\sigma}_{\parallel \text{to} \parallel} |W_2|^2 \right) |X_2|^2 \qquad (6)$$
$$\left. + 4\bar{\sigma}_{\Delta} \text{ Re } (W_1 W_2^*) \text{ Re } (X_1 X_2^*) \right\} ,$$

$$\bar{\sigma}_x = \frac{N}{(1 + |Q_T|^2)(1 + |Q_R|^2)} \left\{ \left(\bar{\sigma}_{\perp \text{to} \perp} |W_2|^2 + \bar{\sigma}_{\perp \text{to} \parallel} |W_1|^2 \right) |X_1|^2 \right.$$
$$+ \left(\bar{\sigma}_{\perp \text{to} \parallel} |W_2|^2 + \bar{\sigma}_{\parallel \text{to} \parallel} |W_1|^2 \right) |X_2|^2 \qquad (7)$$
$$\left. - 4\bar{\sigma}_{\Delta} \text{ Re } (W_1 W_2^*) \text{ Re } (X_1 X_2^*) \right\} ,$$

where Re(·) represents the real part of the quantity in parentheses, * denotes complex conjugation, and

$$X_1 = T_1 - T_2 Q_T \qquad (8)$$

$$X_2 = T_2 + T_1 Q_T \qquad (9)$$

$$T_1 = \sin \theta_2 \sin (\phi_1 - \phi_2)/\sin \beta \qquad (10)$$

$$T_2 = [\sin \theta_1 \cos \theta_2 - \cos \theta_1 \sin \theta_2 \cos (\phi_1 - \phi_2)]/\sin \beta \qquad (11)$$

$$W_1 = R_1 - R_2 Q_R \qquad (12)$$

$$W_2 = R_2 + R_1 Q_R \qquad (13)$$

$$R_1 = \sin \theta_1 \sin (\phi_1 - \phi_2)/\sin \beta \qquad (14)$$

$$R_2 = -[\sin \theta_2 \cos \theta_1 - \cos \theta_2 \sin \theta_1 \cos (\phi_1 - \phi_2)]/\sin \beta \; . \qquad (15)$$

N is the number of dipoles being illuminated by the transmitter that exists in the volume viewed by the receiver's antenna, and $\bar{\sigma}_{\perp \text{to} \perp}$, $\bar{\sigma}_{\parallel \text{to} \parallel}$, $\bar{\sigma}_{\perp \text{to} \parallel}$, and $\bar{\sigma}_{\Delta}$ are four functions (actually are cross sections--see text) that are defined, graphed (figures 3 through 6), and tabularized (tables 1 through 3) in the subsequent text. It results that these four functions depend only on β (for a given dipole length) and are independent of other scattering geometry involving r_1, θ_1, ϕ_1, r_2, θ_2, and ϕ_2.

For a given problem where the geometry is given such that r_1, θ_1, ϕ_1, r_2, θ_2, ϕ_2, β, N, and λ are known, the use of equations (6) and (7) involves mainly two things. First, for whatever dipole case is of interest, the functions $\bar{\sigma}_{\perp to \perp}$, $\bar{\sigma}_{\parallel to \parallel}$, $\bar{\sigma}_{\perp to \parallel}$, and $\bar{\sigma}_{\Delta}$ are determined either from the tables or from the graphs given. Second, Q_T and Q_R must be specified for the transmitter and receiver. Table A-1 (appendix A) is helpful in choosing the Q's for the more common cases. In the general case of elliptical polarizations the relationships of appendix A may be used.

3. ANALYSIS OF SINGLE DIPOLE SCATTERING

The overall scattering geometry is given in figure 1. By proper choice of coordinates defining scattering by the dipole at point D, the effect of the dipole can be separated from the incident path parameters r_1, θ_1, ϕ_1 and the scattering path parameters r_2, θ_2, and ϕ_2. The choice consists of defining a scattering plane TDR. The scattering plane and dipole geometry are shown in figure 2. A coordinate system x', y', z' is defined such that x' and y' axes lie in the plane TDR with x' positioned to bisect the scattering angle β. The dipole is located at the origin of the primed coordinate system with its wire axis located by spherical angles θ_d and ϕ_d, as shown.

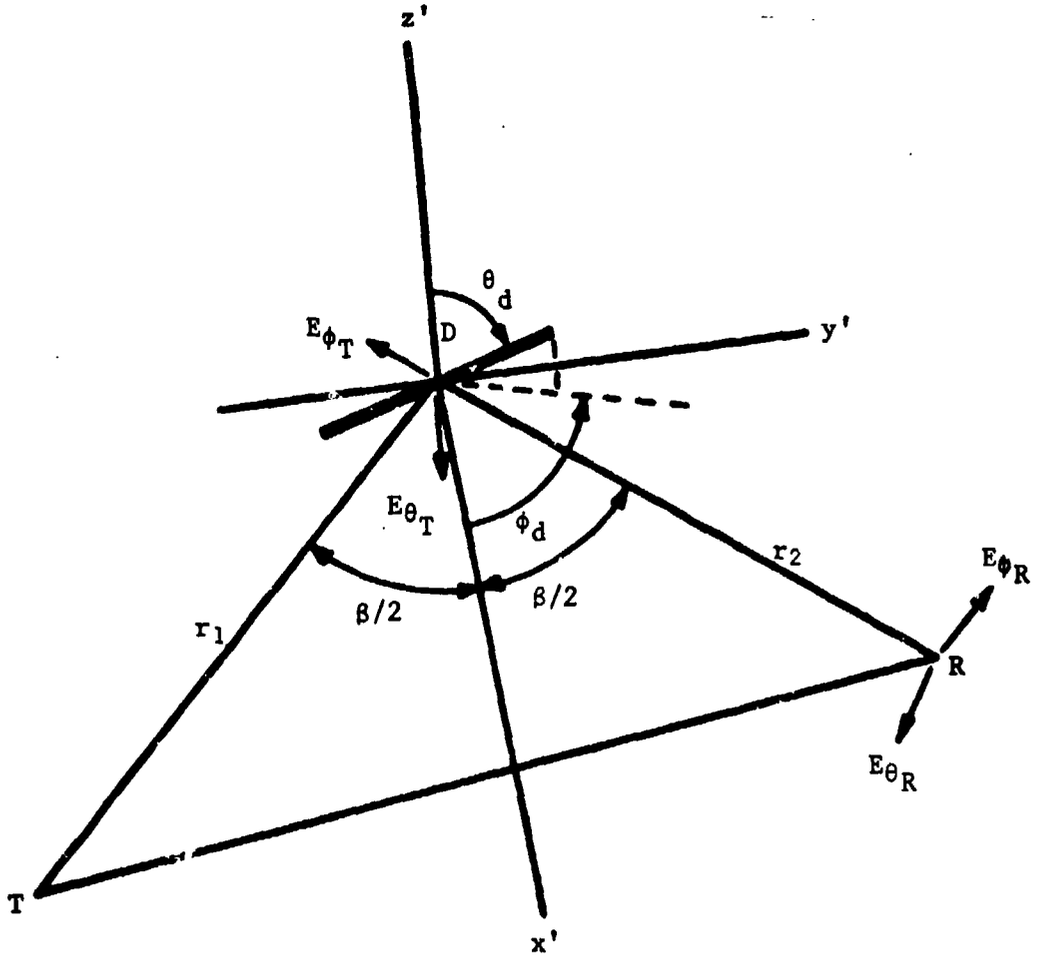

Figure 2. Scattering plane and dipole geometry.

We define $E_{\phi T}$ and $E_{\phi R}$ as incident and received electric field components that lie in the scattering plane and are normal to axes TD and DR, respectively. Similarly we define field components $E_{\theta T}$ and $E_{\theta R}$ that are normal to the scattering plane and orthogonal to $E_{\phi T}$ and $E_{\phi R}$, respectively, all as shown in figure 2. By using the polarization scattering matrix approach to the scattering problem, we have

$$\begin{bmatrix} E_{\theta R} \\ E_{\phi R} \end{bmatrix} = \begin{bmatrix} d_{11} & d_{12} \\ d_{21} & d_{22} \end{bmatrix} \begin{bmatrix} E_{\theta T} \\ E_{\phi T} \end{bmatrix} = [d] \begin{bmatrix} E_{\theta T} \\ E_{\phi T} \end{bmatrix} . \tag{16}$$

Here [d] is the scattering matrix of the dipole with elements d_{mn} that are to be determined, where m and n = 1, 2.

The field components $E_{\theta T}$ and $E_{\phi T}$ are related to the transmitted fields $E_{\theta 1}$ and $E_{\phi 1}$ (figure 1) that are incident on the dipole by

$$\begin{bmatrix} E_{\theta T} \\ E_{\phi T} \end{bmatrix} = \begin{bmatrix} T_{11} & T_{12} \\ T_{21} & T_{22} \end{bmatrix} \begin{bmatrix} E_{\theta 1} \\ E_{\phi 1} \end{bmatrix} = [T] \begin{bmatrix} E_{\theta 1} \\ E_{\phi 1} \end{bmatrix} , \tag{17}$$

where [T] is a field transformation matrix for the incident path that we subsequently determine. In an analogous manner, fields $E_{\theta 2}$ and $E_{\phi 2}$ (figure 1) at the receiver are related to $E_{\theta R}$ and $E_{\phi R}$ by

$$\begin{bmatrix} E_{\theta 2} \\ E_{\phi 2} \end{bmatrix} = \begin{bmatrix} R_{11} & R_{12} \\ R_{21} & R_{22} \end{bmatrix} \begin{bmatrix} E_{\theta R} \\ E_{\phi R} \end{bmatrix} = [R] \begin{bmatrix} E_{\theta R} \\ E_{\phi R} \end{bmatrix} , \tag{18}$$

where [R] is another field transformation matrix for the receiver path. By combining equations (16) through (18) we have

$$\begin{bmatrix} E_{\theta 2} \\ E_{\phi 2} \end{bmatrix} = [R][d][T] \begin{bmatrix} E_{\theta 1} \\ E_{\phi 1} \end{bmatrix} . \tag{19}$$

It is shown in appendix A that the received wave can be decomposed into two elliptically polarized waves. One, with electric field vector we denote by $\vec{E}_{R_1}$, will have an "amplitude" denoted by E_{R_1} and polarization set by Q_R, which is that of the receiver antenna's polarization. The second wave, with electric field vector denoted by $\vec{E}_{R_2}$, has the polarization orthogonal to that of the receiver. Thus, from appendix A, we write

$$\begin{bmatrix} E_{\theta_2} \\ E_{\phi_2} \end{bmatrix} = \vec{E}_{R_1} + \vec{E}_{R_2} = \begin{bmatrix} E_{R_1} \\ E_{R_1} Q_R \end{bmatrix} + \begin{bmatrix} -E_{R_2} Q_R^* \\ E_{R_2} \end{bmatrix} \quad . \tag{20}$$

In a similar manner the transmitted wave's electric field vector, denoted by $\vec{E}_1$, incident at the dipole can be written as

$$\vec{E}_1 = \begin{bmatrix} E_{\theta_1} \\ E_{\phi_1} \end{bmatrix} = \begin{bmatrix} E_T \\ E_T Q_T \end{bmatrix} \quad , \tag{21}$$

where its "amplitude" is[†] E_T and its polarization is determined by Q_T.

By combining equations (20) and (21) with (19) we have

$$\begin{bmatrix} E_{R_1} \\ E_{R_2} \end{bmatrix} = \frac{1}{1 + |Q_R|^2} \begin{bmatrix} 1 & Q_R^* \\ -Q_R & 1 \end{bmatrix} [R][d][T] \begin{bmatrix} 1 \\ Q_T \end{bmatrix} E_T \quad . \tag{22}$$

From appendix A the power in the received fields in the antenna's preferred polarization is proportional to $|\vec{E}_{R_1}|^2 = (1 + |Q_R|^2)|E_{R_1}|^2$; the corresponding result for the orthogonal wave is $|\vec{E}_{R_2}|^2 = (1 + |Q_R|^2)|E_{R_2}|^2$. At the dipole, power in the incident wave is proportional to $|\vec{E}_1|^2 = (1 + |Q_T|^2)|E_T|^2$. From equations (4) and (5) cross sections become

$$\bar{\sigma} = \frac{4\pi r_2^2 (1 + |Q_R|^2)}{(1 + |Q_T|^2)} \frac{E[|E_{R_1}|^2]}{|E_T|^2} \quad , \tag{23}$$

$$\bar{\sigma}_x = \frac{4\pi r_2^2 (1 + |Q_R|^2)}{(1 + |Q_T|^2)} \frac{E[|E_{R_2}|^2]}{|E_T|^2} \quad . \tag{24}$$

[†] E_T is a complex "amplitude" and contains a factor $\exp(-j2\pi r_1/\lambda)$ which accounts for incident-path phase.

Thus, by solving equation (22) we obtain average bistatic cross sections from equations (23) and (24); its solution requires that we first determine matrices [R], [T], and [d].

3.1 Determination of Matrices [R] and [T]

Although we shall omit details because the procedures are straight forward, it is relatively easy to show that

$$[T] = \begin{bmatrix} T_1 & -T_2 \\ T_2 & T_1 \end{bmatrix} , \tag{25}$$

where

$$T_1 = \sin\theta_2 \sin(\phi_1 - \phi_2)/\sin\beta , \tag{26}$$

$$T_2 = [\sin\theta_1 \cos\theta_2 - \cos\theta_1 \sin\theta_2 \cos(\phi_1 - \phi_2)]/\sin\beta , \tag{27}$$

and

$$[R] = \begin{bmatrix} R_1 & R_2 \\ -R_2 & R_1 \end{bmatrix} , \tag{28}$$

where

$$R_1 = \sin\theta_1 \sin(\phi_1 - \phi_2)/\sin\beta , \tag{29}$$

$$R_2 = -[\sin\theta_2 \cos\theta_1 - \cos\theta_2 \sin\theta_1 \cos(\phi_1 - \phi_2)]/\sin\beta . \tag{30}$$

3.2 Dipole Scattering Matrix [d]

Let the dipole be located as shown in the primed coordinate system of figure 2. Let θ and ϕ be angles in spherical coordinates locating an arbitrary direction of interest. Then for a dipole with a sinusoidal current distribution with current I_T in its center (terminal area if it were a center-fed dipole), the effective lengths in directions θ and ϕ, denoted by h_θ and h_ϕ, are known (see Cross [35]) to be

$$[h_\theta \;\; h_\phi] = A(\theta, \phi) \cdot [-\sin\theta \cos\theta_d + \cos\theta \sin\theta_d \cos(\phi - \phi_d) \quad \sin\theta_d \sin(\phi_d - \phi)] , \tag{31}$$

where we define

$$A(\theta, \phi) \triangleq \frac{(\lambda/\pi)}{\sin(\pi L/\lambda)} \cdot \frac{\cos[(\pi L/\lambda)\cos\psi] - \cos(\pi L/\lambda)}{\sin^2\psi} \tag{32}$$

and

$$\cos\psi = \cos\theta\cos\theta_d + \sin\theta\sin\theta_d\cos(\phi - \phi_d) \ . \tag{33}$$

For the special definition of coordinates we employ, the two directions of interest, to receiver and to transmitter, lie in the x',y' plane, so $\theta = \pi/2$ and we have

$$[h_\theta \quad h_\phi] = A\left(\frac{\pi}{2}, \phi\right)[-\cos\theta_d \quad \sin\theta_d \sin(\phi_d - \phi)] \ , \tag{34}$$

where

$$\cos\psi = \sin\theta_d\cos(\phi - \phi_d) \ . \tag{35}$$

For a radiating dipole the electric fields are also known (see Cross [35] p. 15). Our dipole radiates toward point R located at $(r_2, \pi/2, \beta/2)$ from figure 2. The fields at point R become

$$\begin{bmatrix} E_{\theta R} \\ E_{\phi R} \end{bmatrix} = \frac{-j\eta I_T}{2\lambda r_2} e^{-j2\pi r_2/\lambda} \begin{bmatrix} h_\theta(\pi/2, \beta/2) \\ h_\phi(\pi/2, \beta/2) \end{bmatrix} \ , \tag{36}$$

where $\eta = 120\pi$ is the intrinsic impedance of our medium, considered the same as free space. The radiated fields are due to the current induced into the dipole by the incident field. This current is the ratio of induced open-circuit equivalent voltage, denoted by V_{oc}, to antenna impedance, denoted by z_{rad}, when the "load" on the antenna as a receiver is zero (shorted dipole). We have

$$\begin{aligned} I_T &= V_{oc}/z_{rad} \\ &= [E_{\theta T}h_\theta(\pi/2, -\beta/2) - E_{\phi T}h_\phi(\pi/2, -\beta/2)]/z_{rad} \ . \end{aligned} \tag{37}$$

By combining equations (37) and (36) and writing the result in the form of equation (16), we have the elements of [d],

$$d_{11} = BA_0(\beta/2)\cos^2\theta_d \tag{38a}$$

$$d_{12} = BA_0(\beta/2)\cos\theta_d \sin\theta_d \sin(\phi_d + \tfrac{\beta}{2}) \tag{38b}$$

$$d_{21} = -BA_0(\beta/2)\cos\theta_d \sin\theta_d \sin(\phi_d - \tfrac{\beta}{2}) \tag{38c}$$

$$d_{22} = -BA_0(\beta/2)\sin^2\theta_d \sin(\phi_d - \tfrac{\beta}{2}) \sin(\phi_d + \tfrac{\beta}{2}) \ , \tag{38d}$$

where we define

$$B \triangleq [-j\eta/(2\lambda z_{rad} r_2)] \exp(-j2\pi r_2/\lambda) \ , \tag{39}$$

$$A_0(\beta/2) \triangleq A(\pi/2, \beta/2)A(\pi/2, -\beta/2) \ . \tag{40}$$

3.3 Bistatic Cross Sections

Average cross sections can now be found from equations (23) and (24) using equation (22) since matrices [R], [T], and [d] are now defined. Considerable detail is involved, so only the procedure is outlined. If we define two matrices according to

$$\boxed{[X] = \begin{bmatrix} X_1 \\ X_2 \end{bmatrix} = \begin{bmatrix} T_1 - T_2 Q_T \\ T_2 + T_1 Q_T \end{bmatrix}} \tag{41}$$

and

$$\boxed{[W] = \begin{bmatrix} W_1 \\ W_2 \end{bmatrix} = \begin{bmatrix} R_1 - R_2 Q_R \\ R_2 + R_1 Q_R \end{bmatrix}} \ , \tag{42}$$

then E_{R_1} from equation (22) becomes

$$E_{R_1} = \frac{E_T}{1 + |Q_R|^2} [W^*]^t [d][X] \ . \tag{43}$$

Here $[\cdot]^t$ denotes the matrix transpose.

The result of forming $|E_{R_1}|^2$ by using equation (43) and expanding out the matrices is a linear sum of terms involving all possible combinations of the coefficients of [d] with themselves conjugated. When the average $E[|E_{R_1}|^2]$ is formed, assuming angles θ_d and ϕ_d are uniformly distributed in direction over the sphere, the following averages of the coefficient products result:

$$E[d_{11}d_{11}^*] \neq 0 \tag{44a}$$

$$E[d_{11}d_{12}^*] = E[d_{12}d_{11}^*] = 0 \tag{44b}$$

$$E[d_{11}d_{21}^*] = E[d_{21}d_{11}^*] = 0 \tag{44c}$$

$$E[d_{11}d_{22}^*] = E[d_{22}d_{11}^*] = E[d_{12}d_{21}^*] = E[d_{21}d_{12}^*] \neq 0 \tag{44d}$$

$$E[d_{12}d_{12}^*] = E[d_{21}d_{21}^*] \neq 0 \tag{44e}$$

$$E[d_{12}d_{22}^*] = E[d_{22}d_{12}^*] = 0 \tag{44f}$$

$$E[d_{21}d_{22}^*] = E[d_{22}d_{21}^*] = 0 \tag{44g}$$

$$E[d_{22}d_{22}^*] \neq 0 \quad . \tag{44h}$$

The four nonzero quantities in equations (44) are summarized below with appropriate symbol definitions

$$\bar{\sigma}_{\perp \text{to} \perp} \triangleq 4\pi r_2^2 E[d_{11}d_{11}^*] = 4\pi r_2^2 |B|^2 E[A_0^2(\theta_d, \phi_d) \cos^4 \theta_d] \ , \tag{45}$$

$$\begin{aligned} \bar{\sigma}_{\perp \text{to} \parallel} &\triangleq 4\pi r_2^2 E[d_{12}d_{12}^*] \\ &= 4\pi r_2^2 |B|^2 E[A_0^2(\theta_d, \phi_d) \cos^2 \theta_d \sin^2 \theta_d \sin^2 (\phi_d + \tfrac{\beta}{2})] , \end{aligned} \tag{46}$$

$$\begin{aligned} \bar{\sigma}_{\Delta} &\triangleq 4\pi r_2^2 E[d_{11}d_{22}^*] \\ &= -4\pi r_2^2 |B|^2 E[A_0^2(\theta_d, \phi_d) \cos^2 \theta_d \sin^2 \theta_d \sin(\phi_d - \tfrac{\beta}{2}) \sin(\phi_d + \tfrac{\beta}{2})] , \end{aligned} \tag{47}$$

$$\begin{aligned} \bar{\sigma}_{\parallel \text{ to} \parallel} &\triangleq 4\pi r_2^2 E[d_{22}d_{22}^*] \\ &= 4\pi r_2^2 |B|^2 E[A_0^2(\theta_d, \phi_d) \sin^4 \theta_d \sin^2(\phi_d - \tfrac{\beta}{2}) \sin^2(\phi_d + \tfrac{\beta}{2})] , \end{aligned} \tag{48}$$

where the spherical average is defined by

$$E[\cdot] = \frac{1}{4\pi} \int_{\phi_d=0}^{2\pi} \int_{\theta_d=0}^{\pi} [\cdot] \sin \theta_d \, d\theta_d d\phi_d \ . \tag{49}$$

With these definitions $E[|E_{R_1}|^2]$ from equation (43) reduces to a reasonable number of terms, and, when it is substituted into equation (23) we finally obtain

$$\bar{\sigma} = \frac{1}{(1 + |Q_T|^2)(1 + |Q_R|^2)} \Big\{ \big(\bar{\sigma}_{\perp \text{to} \perp} |W_1|^2 + \bar{\sigma}_{\perp \text{to} \parallel} |W_2|^2\big)|X_1|^2 + \big(\bar{\sigma}_{\perp \text{to} \parallel} |W_1|^2 + \bar{\sigma}_{\parallel \text{to} \parallel} |W_2|^2\big)|X_2|^2 + 4\bar{\sigma}_{\Delta} \, \text{Re}\big(W_1 W_2^*\big)\text{Re}\big(X_1 X_2^*\big) \Big\} . \quad (50)$$

If one repeats the above procedure, the average bistatic cross section for the orthogonal receiver polarization becomes

(51)

$$\bar{\sigma}_x = \frac{1}{(1 + |Q_T|^2)(1 + |Q_R|^2)} \Big\{ \big(\bar{\sigma}_{\perp \text{to} \perp} |W_2|^2 + \bar{\sigma}_{\perp \text{to} \parallel} |W_1|^2\big)|X_1|^2 + \big(\bar{\sigma}_{\perp \text{to} \parallel} |W_2|^2 + \bar{\sigma}_{\parallel \text{to} \parallel} |W_1|^2\big)|X_2|^2 - 4\bar{\sigma}_{\Delta} \, \text{Re}(W_1 W_2^*)\text{Re}(X_1 X_2^*) \Big\} .$$

The use of equations (50) and (51) in a given problem amounts to using specified transmitter and receiver antenna polarizations (they determine Q_T and Q_R), using specified geometry (which determines X_1, X_2, W_1, and W_2), and finding the functions $\bar{\sigma}_{\perp \text{to} \perp}$, $\bar{\sigma}_{\perp \text{to} \parallel}$, $\bar{\sigma}_{\Delta}$, and $\bar{\sigma}_{\parallel \text{to} \parallel}$. We next determine these functions.

3.4 Scattering Plane Cross Sections

It is easy to show (examples 1 through 6 below) that if transmitter, dipole, and receiver all lie in the x,y plane of figure 1, then $\bar{\sigma}_{\perp \text{to} \perp}$ is the bistatic cross section when both transmitter and receiver antennas have linear polarization perpendicular to the scattering plane. Similarly, $\bar{\sigma}_{\parallel \text{to} \parallel}$ applies when both are linear and parallel to the scattering plane, while $\bar{\sigma}_{\perp \text{to} \parallel}$ is cross section when both are linear with one parallel and the other perpendicular. Which is which in the last case is not important since it can be shown that $\bar{\sigma}_{\perp \text{to} \parallel} = \bar{\sigma}_{\parallel \text{to} \perp}$. We also show below that $\bar{\sigma}_{\Delta}$ is one half of the difference between $\bar{\sigma}$ and $\bar{\sigma}_x$ when the transmitter and preferred receiver polarizations are linear and tilted 45° from the horizontal axis.

Since the four cross sections given by equations (45) through (48) are, in general, difficult to analytically solve, it is fortunate that they depend only on β and the dipole's length relative to λ.† This fact allows equations (45)

†z_{rad} required in equation (39) is set once L/λ is chosen.

through (48) to be computed by digital computer for various values of β for selected dipole lengths and the results used for any general scattering problem through equations (50) and (51). Computed results are plotted in figures 3, 4, 5, and 6 for dipoles of resonant lengths of $\lambda/2$, λ, and $3\lambda/2$. The numerical data used in the plots are given in tables 1, 2, and 3. For $L = \lambda/2$ the well-known value $z_{rad} = 73.0\Omega$ was used. For $L = 3\lambda/2$ the impedance procedure of Kraus [34, p. 143] was extended to obtain $z_{rad} = 105.4\Omega$. For $L = \lambda$ our model contains an indeterminate form, since $\sin(\pi L/\lambda) = 0$ in equation (32) while $z_{rad} = \infty$ in equation (37), theoretically; in this case it is reasonable that the form of the scattering determined by equations (36) and (37) remains valid except for unknown scale. Scale was arbitrarily set to Chu's value of $0.166\lambda^2$ for the backscatter point, $\beta = 0$; this operation was equivalent to assuming $z_{rad} \sin(\pi L/\lambda) = 224.6\Omega$ in the model.

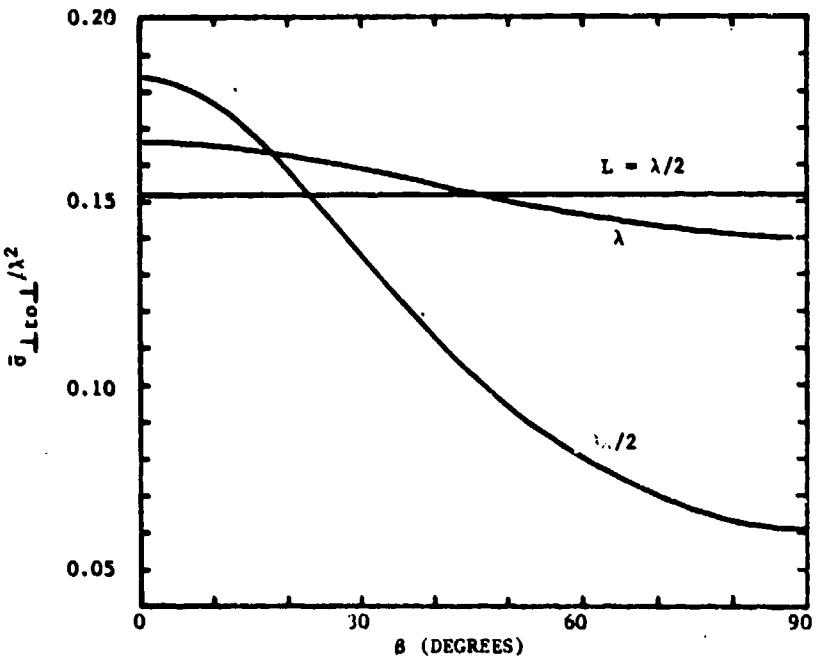

Figure 3. Spherically averaged bistatic cross sections for linear transmitting and receiving polarizations perpendicular to the scattering plane. Cross sections have even symmetry about $\beta = \pi/2$ (90°) and $\beta = \pi$ (180°).

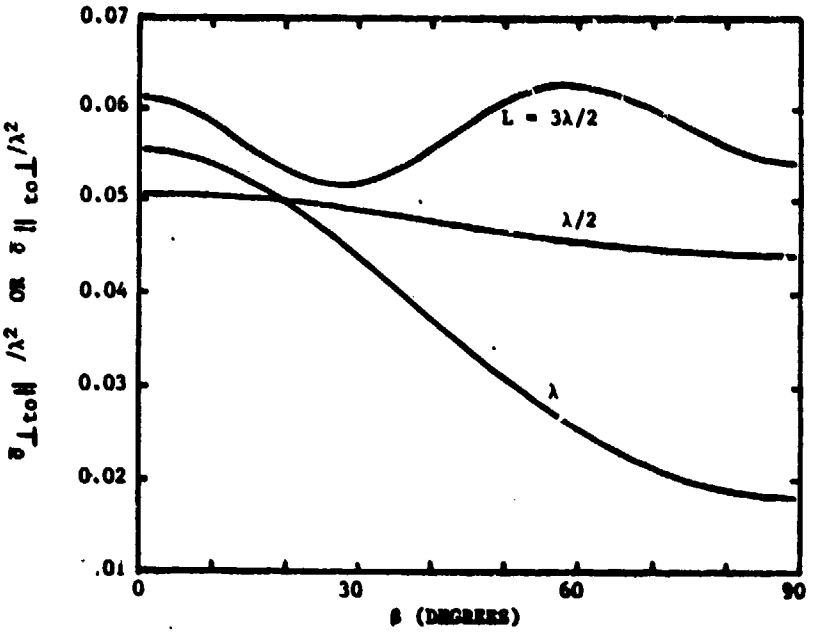

Figure 4. Spherically averaged bistatic cross sections for linear transmitting and receiving polarizations, one perpendicular to and one parallel with the scattering plane. Cross sections have even symmetry about $\beta = \pi/2$ (90°) and $\beta = \pi$ (180°).

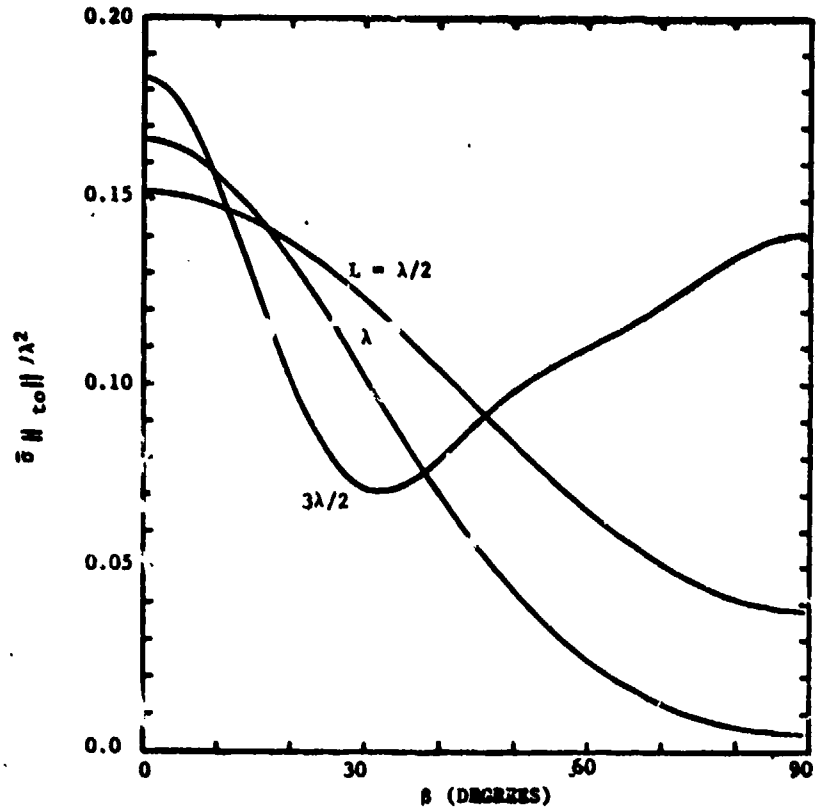

Figure 5. Spherically averaged bistatic cross sections for linear transmitting and receiving polarizations parallel to the scattering plane. Cross sections have even symmetry about $\beta = \pi/2$ (90°) and $\beta = \pi$ (180°).

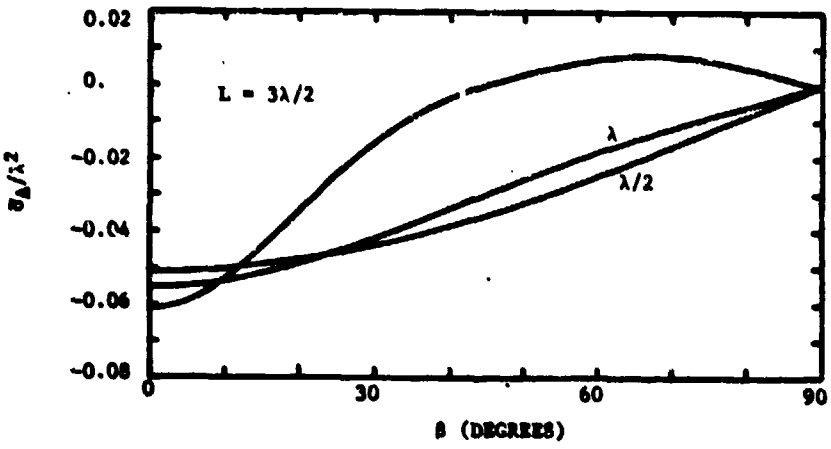

Figure 6. Plots of the function $\bar{\sigma}_\Delta/\lambda^2$ versus bistatic scattering angle β. The function has odd symmetry about $\beta = \pi/2$ (90°) and even symmetry about $\beta = \pi$ (180°).

TABLE 1. FUNCTIONS $\bar{\sigma}_{\perp to \perp}/\lambda^2$, $\bar{\sigma}_{\perp to \parallel}/\lambda^2$, $\bar{\sigma}_{\parallel to \parallel}/\lambda^2$, AND $\bar{\sigma}_\Delta/\lambda^2$ FOR DIPOLE LENGTH L = λ/2 AND VARIOUS VALUES OF BISTATIC SCATTERING ANGLE β.†

β (DEGREES)	$\bar{\sigma}_{\perp to \perp}/\lambda^2$	$\bar{\sigma}_{\perp to \parallel}/\lambda^2$	$\bar{\sigma}_{\parallel to \parallel}/\lambda^2$	$\bar{\sigma}_\Delta/\lambda^2$
0	0.15203	0.05067	0.15202	-0.05067
5	0.15202	0.05062	0.15113	-0.05047
10	0.15200	0.05047	0.14847	-0.04987
15	0.15196	0.05022	0.14415	-0.04888
20	0.15192	0.04988	0.13830	-0.04751
25	0.15186	0.04947	0.13112	-0.04577
30	0.15179	0.04899	0.12283	-0.04367
35	0.15171	0.04846	0.11371	-0.04125
40	0.15163	0.04789	0.10405	-0.03851
45	0.15155	0.04731	0.09415	-0.03549
50	0.15146	0.04673	0.08430	-0.03221
55	0.15138	0.04617	0.07481	-0.02869
60	0.15131	0.04564	0.06596	-0.02498
65	0.15124	0.04517	0.05780	-0.02108
70	0.15118	0.04476	0.05116	-0.01074
75	0.15113	0.04443	0.04563	-0.01288
80	0.15110	0.04419	0.04157	-0.00864
85	0.15108	0.04404	0.03909	-0.00433
90	0.15107	0.04399	0.03826	0.0

†All functions have even symmetry about β = 90 deg and β = 180 deg except $\bar{\sigma}_\Delta/\lambda^2$, which has odd symmetry about β = 90 deg and even symmetry about β = 180 deg.

TABLE 2. FUNCTIONS $\bar{\sigma}_{\perp to \perp}/\lambda^2$, $\bar{\sigma}_{\perp to \parallel}/\lambda^2$, $\bar{\sigma}_{\parallel to \parallel}/\lambda^2$, AND $\bar{\sigma}_{\Delta}/\lambda^2$ FOR DIPOLE LENGTH L = λ AND VARIOUS VALUES OF BISTATIC SCATTERING ANGLE β.†

β (DEGREES)	$\bar{\sigma}_{\perp to \perp}/\lambda^2$	$\bar{\sigma}_{\perp to \parallel}/\lambda^2$	$\bar{\sigma}_{\parallel to \parallel}/\lambda^2$	$\bar{\sigma}_{\Delta}/\lambda^2$
0	0.16600	0.05532	0.16597	-0.05532
5	0.16579	0.05495	0.16375	-0.05490
10	0.16515	0.05386	0.15728	-0.05364
15	0.16412	0.05211	0.14705	-0.05162
20	0.16272	0.04979	0.13385	-0.04893
25	0.16103	0.04702	0.11862	-0.04568
30	0.15909	0.04392	0.10236	-0.04202
35	0.15698	0.04064	0.08602	-0.03809
40	0.15477	0.03729	0.07042	-0.03402
45	0.15253	0.03402	0.05618	-0.02992
50	0.15033	0.03091	0.04370	-0.02589
55	0.14824	0.02805	0.03317	-0.02202
60	0.14631	0.02551	0.02461	-0.01833
65	0.14459	0.02332	0.01791	-0.01485
70	0.14313	0.02151	0.01286	-0.01158
75	0.14197	0.02010	0.00924	-0.00850
80	0.14111	0.01909	0.00684	-0.00558
85	0.14060	0.01848	0.00547	-0.00276
90	0.14042	0.01828	0.00503	0.0

†All functions have even symmetry about β = 90 deg and β = 180 deg except $\bar{\sigma}_{\Delta}/\lambda^2$, which has odd symmetry about β = 90 deg and even symmetry about β = 180 deg.

TABLE 3. FUNCTIONS $\bar{\sigma}_{\perp to \perp}/\lambda^2$, $\bar{\sigma}_{\perp to \parallel}/\lambda^2$, $\bar{\sigma}_{\parallel to \parallel}/\lambda^2$, AND $\bar{\sigma}_{\Delta}/\lambda^2$ FOR DIPOLE LENGTH L = $3\lambda/2$ AND VARIOUS VALUES OF BISTATIC SCATTERING β.†

β (DEGREES)	$\bar{\sigma}_{\perp to \perp}/\lambda^2$	$\bar{\sigma}_{\perp to \parallel}/\lambda^2$	$\bar{\sigma}_{\parallel to \parallel}/\lambda^2$	$\bar{\sigma}_{\Delta}/\lambda^2$
0	0.18369	0.06121	0.18363	-0.06121
5	0.18188	0.06044	0.17585	-0.05918
10	0.17663	0.05840	0.15494	-0.05345
15	0.16850	0.05574	0.12718	-0.04501
20	0.15827	0.05331	0.10032	-0.03519
25	0.14681	0.05189	0.08078	-0.02534
30	0.13499	0.05189	0.07165	-0.01649
35	0.12349	0.05332	0.07232	-0.00924
40	0.11278	0.05574	0.07950	-0.00371
45	0.10311	0.05851	0.08914	+0.00033
50	0.09455	0.06089	0.09808	0.00324
55	0.08703	0.06235	0.10504	0.00534
60	0.08047	0.06261	0.11044	0.00678
65	0.07480	0.06173	0.11552	0.00761
70	0.07000	0.06000	0.12131	0.00766
75	0.06611	0.05790	0.12790	0.00685
80	0.06326	0.05594	0.13436	0.00518
85	0.06144	0.05457	0.13915	+0.00279
90	0.06084	0.05407	0.14093	0.0

†All functions have even symmetry about β = 90 deg and β = 180 deg except $\bar{\sigma}_{\Delta}/\lambda^2$, which has odd symmetry about β = 90 deg and even symmetry about β = 180 deg.

Data for $L = \lambda/2$ agree well with those of Mack and Reiffen [21]. However, data for $L = \lambda$ do not agree with those in [21] because of an error recently confirmed by Reiffen [36]; the error appears to stem from an erroneous equation (eq. (10) in [21]) used in computer simulation. The error has apparently never been corrected in the literature and it has been propagated [6, p. 302].

3.5 Relationship to Stokes' Parameter Method

As mentioned previously, the analysis of Dedrick, Hessing, and Johnson [30] using Stokes' parameters showed that only four parameters denoted by $\langle \sigma M_{11} \rangle$, $\langle \sigma M_{12} \rangle$, $\langle \sigma M_{22} \rangle$, and $\langle \sigma M_{33} \rangle$ are needed to find cross sections for any polarizations of transmission and reception. Unfortunately, their work related to polarizations defined with respect to the scattering plane, and general relations for geometry such as in figure 1 were not developed. Also, their evaluations of the four functions were not done for the usual resonant dipole lengths. Furthermore, their numerical work relied on a computer integration method that produced significant error (observe fluctuations in their plotted data). We can show that these difficulties are all overcome by use of the present results. The procedure is simply to show how the four functions of Dedrick et al. [30] are related to the four cross sections found here to be required for the general problem.

Parameters $\bar{\sigma}_{\parallel \text{to} \parallel}$, $\bar{\sigma}_{\perp \text{to} \perp}$, and $\bar{\sigma}_{\perp \text{to} \parallel} = \bar{\sigma}_{\parallel \text{to} \perp}$ here and the respective parameters $\sigma_{\parallel \text{to} \parallel}$, $\sigma_{\perp \text{to} \perp}$, and $\sigma_{\parallel \text{to} \perp}$ of Dedrick et al. [30] are defined identically. Thus, we use the equalities and solve equation (19) of Dedrick et al. [30] to obtain

$$\langle \sigma M_{11} \rangle = \frac{1}{2}(\bar{\sigma}_{\parallel \text{to} \parallel} + 2\bar{\sigma}_{\perp \text{to} \parallel} + \bar{\sigma}_{\perp \text{to} \perp}) , \tag{52}$$

$$\langle \sigma M_{22} \rangle = \frac{1}{2}(\bar{\sigma}_{\parallel \text{to} \parallel} - 2\bar{\sigma}_{\perp \text{to} \parallel} + \bar{\sigma}_{\perp \text{to} \perp}) , \tag{53}$$

$$\langle \sigma M_{12} \rangle = \frac{1}{2}(\bar{\sigma}_{\parallel \text{to} \parallel} - \bar{\sigma}_{\perp \text{to} \perp}) . \tag{54}$$

To show the remaining relationship let $\bar{\sigma}_{/+/}$ denote the value of $\bar{\sigma}$ corresponding to linear transmitted and received preferred polarizations tilted 45° from the respective ϕ_T and ϕ_R axes when T, D, and R all lie in the x,y plane of figure 1. For the same conditions denote the value of $\bar{\sigma}_x$ by $\bar{\sigma}_{/\text{to}\backslash}$. Then it can be shown that

$$\langle \sigma M_{33} \rangle = 2\bar{\sigma}_{\Delta} . \tag{55}$$

4. MULTIPLE DIPOLE SCATTERING

When scattering is due to many, say N, dipoles in a cloud, the received fields are the sums of fields caused by individual dipoles.† For a typical, say the i^{th}, dipole equation (22) again applies, where now all the parameters of [R], [d], [T], Q_T, and even E_T may, in general, depend on i. However, some reasonable assumptions will greatly simplify the developments. Let us assume the dipoles viewed by the transmitter, in its main beam for example, are either far enough away or are of sufficiently small range and angular extent that their incident waves are all of the same polarization and all of about the same field strength ($1/r_1$ factor about the same for all dipoles). These assumptions allow $|E_T|$, Q_T, and [T] to all be approximately independent of i. By making similar assumptions about the cloud-receiver path [R] is approximately independent of i. These assumptions basically make equations (4) and (5) valid provided $|E_{R_1}|^2$ and $|E_{R_2}|^2$ are properly determined; alternatively, equations (23) and (24) are equivalent valid forms.

The, now total, received field "amplitude" components, denoted again by E_{R_1} and E_{R_2}, from equation (22) are††

$$\begin{bmatrix} E_{R_1} \\ E_{R_2} \end{bmatrix} = \frac{1}{1 + |Q_R|^2} \begin{bmatrix} 1 & Q_R^* \\ -Q_R & 1 \end{bmatrix} [R][D][T] \begin{bmatrix} 1 \\ Q_T \end{bmatrix} |E_T| \ , \tag{56}$$

where all terms are defined as before except

$$[D] \triangleq \begin{bmatrix} D_{11} & D_{12} \\ D_{21} & D_{22} \end{bmatrix} = \begin{bmatrix} \sum_{i=1}^{N} d_{11i} e^{-j2\pi r_{1i}/\lambda} & \sum_{i=1}^{N} d_{12i} e^{-j2\pi r_{1i}/\lambda} \\ \sum_{i=1}^{N} d_{21i} e^{-j2\pi r_{1i}/\lambda} & \sum_{i=1}^{N} d_{22i} e^{-j2\pi r_{1i}/\lambda} \end{bmatrix} . \tag{57}$$

---

† We shall assume that scattered fields due to multiple reflections between dipoles are negligible.

†† The phase of E_T has been incorporated into the definition of [D].

Parameters d_{mni} for m and n = 1, 2, are now given by equation (38) with variables θ_d and ϕ_d replaced by θ_{di} and ϕ_{di}, respectively. Variable r_2 in the exponent of equation (39) is replaced by r_{2i}; but, because of the above assumptions, r_2 in the factor $1/r_2$ remains the nominal distance to the cloud and does not depend on i.

The procedure for find $\bar{\sigma}$ and $\bar{\sigma}_x$ proceeds exactly as above for one dipole; we expand equation (56) and obtain $|E_{R1}|^2$ and $|E_{R2}|^2$ so that substitution into equations (23) and (24) can be made. The expansions again lead to ten functions as given in equation (44) except where the D_{mn} replace the d_{mn}, m and n = 1, 2. Expectations now must include the randomness of dipole positions because positions affect the phases of the parameters D_{mn} through factors $\exp[-j2\pi(r_{1i} + r_{2i})/\lambda]$. By making the reasonable assumption that the phases $2\pi(r_{1i} + r_{2i})/\lambda$ are uniformly distributed on (0, 2π) and that dipole phases are independent, due to independent positions, we find the important result that the ten functions of equations (44) involving the D_{mn} are individually equal to the ten functions of equations (44) involving the d_{mn} for a single dipole multiplied by N. Thus, all cross sections based on scattering from the N dipoles are equal simply to N times the cross section of a typical dipole. Dipole cloud cross sections are simply N times the results of equations (50) and (51) which leads finally to equations (6) and (7).

5. SCATTERING EXAMPLES

5.1 Transmitter-Cloud-Receiver in x,y Plane

Several examples serve to illustrate the physical meanings of $\bar{\sigma}_{\perp to \perp}$, $\bar{\sigma}_{\perp to \parallel}$, $\bar{\sigma}_{\parallel to \parallel}$, and $\bar{\sigma}_{\Delta}$. These examples assume the transmitter, the receiver, and the cloud's centroid lie in the x,y plane (figure 1). Thus, $\theta_1 = \pi/2$, $\theta_2 = \pi/2$, $\beta = \phi_2 - \phi_1 - \pi$ and, from equations (8) through (15), we find $T_1 = 1$, $T_2 = 0$, $R_1 = 1$, and $R_2 = 0$, so $X_1 = 1$, $X_2 = Q_T$, $W_1 = 1$, and $W_2 = Q_R$. The reduced forms of equations (6) and (7) become

$$\bar{\sigma} = \frac{N}{(1 + |Q_T|^2)(1 + |Q_R|^2)} \left\{ \bar{\sigma}_{\perp to \perp} + \bar{\sigma}_{\perp to \parallel} (|Q_R|^2 + |Q_T|^2) + \bar{\sigma}_{\parallel to \parallel} |Q_R|^2 |Q_T|^2 + 4\bar{\sigma}_{\Delta} \, Re(Q_R) \, Re(Q_T) \right\} , \tag{58}$$

$$\bar{\sigma}_x = \frac{N}{(1 + |Q_T|^2)(1 + |Q_R|^2)} \left\{ \bar{\sigma}_{\perp to \parallel} (1 + |Q_T|^2 |Q_R|^2) + \bar{\sigma}_{\perp to \perp} |Q_R|^2 + \bar{\sigma}_{\parallel to \parallel} |Q_T|^2 - 4\bar{\sigma}_{\Delta} \, Re(Q_R) \, Re(Q_T) \right\} . \tag{59}$$

A transmitter or receiver having vertical (V) linear polarization has its electric field vector perpendicular ($\perp$) to the scattering plane, while horizontal (H) linear corresponds to a field vector parallel ($\parallel$) to the scattering plane.

Example 1--Transmit V, receive V: From table A-1, $Q_T = 0$, $Q_R = 0$. From equation (58), the cross section, denoted by $\bar{\sigma}_{VV}$, for the preferred receive polarization is

$$\bar{\sigma}_{VV} \triangleq \bar{\sigma} = N\bar{\sigma}_{\perp \text{ to } \perp} . \tag{60}$$

The cross polarization corresponds to reception of H:

$$\bar{\sigma}_{VH} \triangleq \bar{\sigma}_x = N\bar{\sigma}_{\perp \text{ to } \parallel} , \tag{61}$$

from equation (59).

Example 2--Transmit H, receive H: From table A-1, $Q_T = \infty$, $Q_R = \infty$. From equation (58) cross section, $\bar{\sigma}_{HH}$, is

$$\bar{\sigma}_{HH} \triangleq \bar{\sigma} = N\bar{\sigma}_{\parallel \text{ to } \parallel} . \tag{62}$$

Cross polarization, $\bar{\sigma}_{HV}$, from equation (59) becomes

$$\bar{\sigma}_{HV} \triangleq \bar{\sigma}_x = N\bar{\sigma}_{\perp \text{ to } \parallel} = N\bar{\sigma}_{\parallel \text{ to } \perp} . \tag{63}$$

Example 3--Transmit V, receive H: Here $Q_T = 0$, $Q_R = \infty$. Cross sections from equations (58) and (59), denoted by $\bar{\sigma}_{VH}$ and $\bar{\sigma}_{VV}$ become

$$\bar{\sigma}_{VH} \triangleq \bar{\sigma} = N\bar{\sigma}_{\perp \text{ to } \parallel} , \tag{64}$$

$$\bar{\sigma}_{VV} \triangleq \bar{\sigma}_x = N\bar{\sigma}_{\perp \text{ to } \perp} . \tag{65}$$

Example 4--Transmit H, receive V: Here $Q_T = \infty$, $Q_R = 0$. Similar to example 3 we get

$$\bar{\sigma}_{HV} \triangleq \bar{\sigma} = N\bar{\sigma}_{\perp \text{ to } \parallel} = N\bar{\sigma}_{\parallel \text{ to } \perp} , \tag{66}$$

$$\bar{\sigma}_{HH} \triangleq \bar{\sigma}_x = N\bar{\sigma}_{\parallel \text{ to } \parallel} . \tag{67}$$

Example 5--Transmit linear tilted from horizontal by 45°, receive same. Here $Q_T = 1$, $Q_R = -1$. Denote by $N\bar{\sigma}_{/to/}$ the total cross section applicable to the preferred receiver polarization given by equation (58); it is

$$N\bar{\sigma}_{/to/} \triangleq \bar{\sigma} = \frac{N}{4}\left[\bar{\sigma}_{\perp to \perp} + 2\bar{\sigma}_{\perp to \parallel} + \bar{\sigma}_{\parallel to \parallel} + 4\bar{\sigma}_{\Delta}\right] . \tag{68}$$

The cross section, denoted by $N\bar{\sigma}_{/to\backslash}$, for the receiver cross-polarization given by $\bar{\sigma}_x$ is

$$N\bar{\sigma}_{/to\backslash} \triangleq \bar{\sigma}_x = \frac{N}{4}\left[\bar{\sigma}_{\perp to \perp} + 2\bar{\sigma}_{\perp to \parallel} + \bar{\sigma}_{\parallel to \parallel} - 4\bar{\sigma}_{\Delta}\right] . \tag{69}$$

By subtracting equation (69) from equation (68) we get

$$\bar{\sigma}_{\Delta} = \left(\bar{\sigma}_{/to/} - \bar{\sigma}_{/to\backslash}\right)/2 . \tag{70}$$

Thus, $\bar{\sigma}_{\Delta}$ is half the difference in cross sections (per dipole) seen by the receiver in preferred and orthogonal polarizations when transmit and preferred receiver polarizations are linear and tilted 45° with respect to the scattering plane.

By retracing this example, we also find

$$\bar{\sigma}_{\Delta} = \left(\bar{\sigma}_{\backslash to\backslash} - \bar{\sigma}_{\backslash to/}\right)/2 . \tag{71}$$

Example 6--Transmit right-circular, denoted by O_R, receive right-circular. Here $Q_T = -j$, $Q_R = j$ and

$$\bar{\sigma}_{O_R \text{ to } O_R} \triangleq \bar{\sigma} = \left(\bar{\sigma}_{\perp to \perp} + 2\bar{\sigma}_{\perp to \parallel} + \bar{\sigma}_{\parallel to \parallel}\right)N/4 , \tag{72}$$

$$\bar{\sigma}_{O_R \text{ to } O_L} \triangleq \bar{\sigma}_x = \bar{\sigma}_{O_R \text{ to } O_R} , \tag{73}$$

where O_L denotes left-circular. Here we see that a circularly polarized receiver sees the same cross section regardless of choice of rotation sense. Similarly it results that

$$\bar{\sigma}_{O_L \text{ to } O_L} \triangleq \bar{\sigma} = \left(\bar{\sigma}_{\perp to \perp} + 2\bar{\sigma}_{\perp to \parallel} + \bar{\sigma}_{\parallel to \parallel}\right)N/4 , \tag{74}$$

$$\bar{\sigma}_{O_L \text{ to } O_R} \triangleq \bar{\sigma}_x = \bar{\sigma}_{O_L \text{ to } O_L} . \tag{75}$$

Thus, bistatic cross section is the same when both transmitter and receiver have circular polarizations, regardless of combinations of rotation senses.

5.2 Cloud-Receiver Not in x,y Plane, Example 7

As a final example let the transmitter have linear polarization in the θ_1 direction ($Q_T = 0$) and the receiver preferred polarization be linear in the θ_2 direction ($Q_R = 0$). Let the centroid of a cloud of half-wave dipoles be located at $\theta_1 = 25\pi/180$ (or 25°) and $\phi_1 = 75\pi/180$ (or 75°) at a distance $r_1 = 5(10^3)$m. The receiver is at a distance $r_2 = 10^4$ m from the cloud centroid and $12.5(10^3)$m from the transmitter. The receiver has an "elevation" angle of 50° from the x,y plane as seen from the transmitter. We find bistatic cross sections $\bar{\sigma}/(N\lambda^2)$ and $\bar{\sigma}_x/(N\lambda^2)$.

From simple geometry as in figure 1, we find that $\beta = 108.21\pi/180$ (or 108.21°), $\theta_2 = 59.71\pi/180$, $\phi_2 = 321.65\pi/180$, and $\phi_1 - \phi_2 = 113.35\pi/180$. From equations (8) through (15) we calculate $X_1 = T_1 = 0.835$, $X_2 = T_2 = 0.551$, $W_1 = R_1 = 0.408$, and $W_2 = R_2 = -0.913$. By interpolation of table 1 at scattering angle 71.79° [90.0° - (108.21° - 90.0°)] we find $\bar{\sigma}_{\parallel to \parallel}/\lambda^2 = 0.04918$, $\bar{\sigma}_{\perp to \perp}/\lambda^2 = 0.15116$, $\bar{\sigma}_{\perp to \parallel}/\lambda^2 = 0.04464$, and $\bar{\sigma}_\Delta/\lambda^2 = 0.01151$. Finally from equations (6) and (7) we calculate $\bar{\sigma}/(N\lambda^2) = 0.0503$ and $\bar{\sigma}_x/(N\lambda^2) = 0.1146$. Note for this problem's geometry the antenna with preferred polarization would receive less power than one with the orthogonal polarization.

6. SUMMARY AND DISCUSSION

In this paper the spherically averaged bistatic cross sections applicable to a cloud of randomly positioned and randomly oriented resonant dipoles have been found. For a transmitting antenna of arbitrarily specified polarization (set by parameter Q_T as discussed in appendix A), a receiving antenna of arbitrarily specified (by parameter Q_R) polarization, and geometry shown in figure 1, the cross section is given by $\bar{\sigma}$ of (6). The cross section applicable to the corresponding orthogonal receive-antenna polarization is given by $\bar{\sigma}_x$ of equation (7).

Parameters X_1, X_2, W_1, and W_2 depend on the geometry of the problem and are found from equations (8) through (15). The functions $\bar{\sigma}_{\perp to \perp}$, $\bar{\sigma}_{\perp to \parallel}$, $\bar{\sigma}_{\parallel to \parallel}$, and $\bar{\sigma}_\Delta$ depend on the length of the resonant dipole chosen (half-wavelength, full-wavelength, etc.) and on the scattering angle β of figure 1; they are plotted in figures 3 through 6 and tabularized in tables 1, 2, and 3.

Our results agree well with Mack and Reiffen [21] for half-wavelength dipoles, correct erroneous results in [21] for full-wave dipoles, give new results for three-halves-wavelength dipoles, and have produced explicit expressions for cross sections for any geometry. The relationships to another analysis method using Stokes' parameters [30] has been shown, and, by proper use of parameters of this paper, one may compute the parameters of Dedrick et al. [30] with better accuracy.

Equations (6) and (7) were derived assuming perfectly conducting, thin dipoles of resonant length, having a sinusoidal current distribution along their length. Such a distribution is reasonable for shorter wire lengths; it becomes questionable for longer lengths. The model used is therefore probably not applicable for lengths longer than about three-halves wavelength.

ACKNOWLEDGEMENT

The author is grateful to Professor R. C. Johnson, University of Florida. for several helpful discussions.

LITERATURE CITED

[1] Fink, D. G., "Radar Countermeasures," Electronics, Vol. 19, January 1946, pp. 92-97.

[2] DilPare, A. L., "Chaff Primer," Microwaves, Vol. 9, No. 12, December 1970, pp. 46-47.

[3] Puskar, R. J., "Radar Reflector Studies," Proc. of the IEEE 1974 National Aerospace and Electronics Conference, May 13-15, 1974, pp. 177-183.

[4] Sundaram, G. S., "Expendables in Electronic Warfare - Proven Decoys for Survival," International Defense Review, December 1976, pp. 1045-1050.

[5] Butters, B. C. F., "Chaff," IEE Proceedings, Vol. 129, Pt. F, No. 3, June 1982, pp. 197-201.

[6] Ruck, G. T. (Editor), Radar Cross Section Handbook, Vol. 1, Plenum Press, New York, 1970.

[7] Peebles, Peyton Z., Jr., "A Bibliography for Radar Chaff," Harry Diamond Laboratories (U. S. Army) report HDL-CR-83-107-5, September 1983.

[8] Bloch, F., Hamermesh, M., and M. Phillips, "Return Cross Sections from Random Oriented Resonant Half-Wave Length Chaff," Harvard University, Radio Research Laboratory, Technical Memorandum 411-TM-127, June 19, 1944.

[9] Van Vleck, J. H., Bloch, F., and M. Hamermesh, "Theory of Radar Reflection from Wires or Thin Metallic Strips," Journal of Applied Physics, Vol. 18, March 1947, pp. 274-294.

[10] King, R., and D. Middleton, "The Cylindrical Antenna; Current and Impedance," Quarterly of Applied Mathematics, Vol. 3, No. 4, 1946, pp. 302-335.

[11] Tai, C. T., "Electromagnetic Back-Scattering from Cylindrical Wires," Journal of Applied Physics, Vol. 23, August 1952, pp. 909-916.

[12] Cassedy, E. S., and J. Fainberg, "Back Scattering Cross Sections of Cylindrical Wires of Finite Conductivity," IRE Transactions on Antennas and Propagation, Vol. AP-8, No. 1, January 1960, pp. 1-7.

[13] Harrison, C. W., Jr., and R. O. Heinz, "On the Radar Cross Section of Rods, Tubes, and Strips of Finite Conductivity," IEEE Transactions on Antennas and Propagation, Vol. AP-11, No. 4, July 1963, pp. 459-468.

[14] Chen, C-L., "On the Scattering of Electromagnetic Waves from a Long Wire," Radio Science, Vol. 3 (New Series), No. 6, June 1968, pp. 585-598.

[15] Wickliff, R. G., and R. J. Garbacz, "The Average Backscattering Cross Section of Clouds of Randomized Resonant Dipoles," IEEE Transactions on Antennas and Propagation, Vol. AP-22, No. 3, May 1974, pp. 503-505; see also corrections in Vol. AP-22, No. 6, November 1974, pp. 842-843.

[16] Medgyesi-Mitschang, L. N., and C. Eftimiu, "Scattering from Wires and Open Circular Cylinders of Finite Length Using Entire Domain Galerkin Expansions," IEEE Transactions on Antennas and Propagation, Vol. AP-30, No. 4, July 1982, pp. 628-636.

[17] Pyati, V. P., "On the Convergence of the Scattering Statistics of Finite Number of Randomly Oriented Dipoles to Rayleigh," Proceedings of the IEEE, Vol. 63, No. 6, June 1975, pp. 985-986.

[18] Wong, J. L., Reed, I. S., and Z. A. Kaprielian, "A Model for the Radar Echo from a Random Collection of Rotating Dipole Scatterers," IEEE Transactions on Aerospace and Electronic Systems, Vol. AES-2, No. 2, March 1967, pp. 171-178.

[19] Ioannidis, G. A., "Model for Spectral and Polarization Characteristics of Chaff," IEEE Transactions on Aerospace and Electronic Systems, Vol. 5, AES-15, No. 5, September 1979, pp. 723-726.

[20] Hessemer, R. A., Jr., "Scatter Communications with Radar Chaff," IRE Transactions on Antennas and Propagation, Vol. AP-9, No. 2, March 1961, pp. 211-217.

[21] Mack, C. L., Jr., and B. Reiffen, "RF Characteristics of Thin Dipoles," Proceedings of the IEEE, Vol. 52, No. 5, May 1964, pp. 533-542.

[22] Harrington, R. F., "RF Characteristics of Thin Dipoles," Proceedings of the IEEE, Vol. 52, No. 12, December 1964, pp. 1736-1737.

[23] Borison, S. L., "Bistatic Scattering Cross Section of a Randomly-Oriented Dipole," IEEE Transactions on Antennas and Propagation, Vol. AP-15, No. 2, March 1967, pp. 320-321.

[24] Palermo, C. J., and L. H. Bauer, "Bistatic Scattering Cross Section of Chaff Dipoles with Applications to Communications," Proceedings of the IEEE, Vol. 53, No. 8, August 1965, pp. 1119-1121.

[25] DiCaudo, V. J., and W. W. Martin, "Approximate Solution to Bistatic Radar Cross Section of Finite Length, Infinitely Conducting Cylinder," IEEE Transactions on Antennas and Propagation, Vol. AP-14, No. 5, September 1966, pp. 668-669.

[26] Harrington, R. F., and J. R. Mautz, "Straight Wires with Arbitrary Excitation and Loading," IEEE Transactions on Antennas and Propagation, Vol. AP-15, No. 4, July 1967, pp. 502-515.

[27] Breithaupt, R. W., "Bistatic Scattering by a Thin, Lossy Cylindrical Wire," Canadian Journal of Physics, Vol. 45, No. 6, June 1967, pp. 1965-1980.

[28] Einarsson, O., "Electromagnetic Scattering by a Thin Finite Wire," Acta Polytechnica Scandinavica, Electrical Engineering Series No. 23, UDC 538.566, 621.396.67, Stockholm, May 1969.

[29] Garbacz, R. J., Cable, V., Wickliff, R., Caldecott, R., Buk, J., Lam, D., Demarest, K., and A. Yee, "Advanced Radar Reflector Studies," Ohio State University, Electroscience Laboratory, Report AFAL-TR-75-219, December 1975; also DTIC Document No. ADB013005.

[30] Dedrick, K. G., Hessing, A. R., and G. L. Johnson, "Bistatic Radar Scattering by Randomly Oriented Wires," IEEE Transactions on Antennas and Propagation, Vol. AP-26, No. 3, May 1978, pp. 420-426.

[31] Heath, G. E., "Bistatic Scattering Reflection Asymmetry, Polarization Reversal Asymmetry, and Polarization Reversal Reflection Symmetry," IEEE Transactions on Antennas and Propagation, Vol. AP-29, No. 3, May 1981, pp. 429-434.

[32] Heath, G. E., "Properties of the Linear Polarization Bistatic Scattering Matrix," IEEE Transactions on Antennas and Propagation, Vol. AP-29, No. 3, May 1981, pp. 523-525.

[33] FitzGerrell, R. G., "Radiation Efficiencies of Half-Wave Dipole Antennas," IEEE Transactions on Antennas and Propagation, Vol. AP-13, No. 2, March 1965, pp. 326-327.

[34] Kraus, J. D., Antennas, McGraw-Hill Book Co., New York, NY, 1950.

[35] Cross, J. L., "Response of Arrays to Stochastic Fields," Ph.D. Dissertation, University of Florida, Gainesville, FL, 1969.

[36] Reiffen, B., private communication.

[37] Beckmann, P., and A. Spizzichino, The Scattering of Electromagnetic Waves from Rough Surfaces, The MacMillian Co., New York, NY, 1963.

APPENDIX A--POLARIZATION CONSIDERATIONS

A general, elliptically polarized, plane wave propagating in the r direction has electric field components E_θ and E_ϕ in the θ and ϕ directions at the origin of a spherical coordinate system given by Kraus [34]:

$$E_\theta = A \cos \omega t = \mathrm{Re}\left(A\, e^{j\omega t}\right), \tag{A-1}$$

$$E_\phi = B \cos(\omega t + \alpha) = \mathrm{Re}\left(B\, e^{j\omega t + j\alpha}\right). \tag{A-2}$$

Here A and B are peak amplitudes (positive quantities), α is a phase angle, ω is angular frequency, and t is time. The wave is completely specified by the three quantities A, B, and α. For an observer at the origin looking in the direction of propagation, the instantaneous electric field vector appears to rotate in a counter-clockwise direction for $0 < \alpha < \pi$ regardless of the relative amplitudes of A and B; this is defined as left-elliptical polarization by IEEE standards. For $-\pi < \alpha < 0$ rotation is clockwise and we have right-elliptical polarization. If A = B the locus of the tip of the electric field vector is a circle when $\alpha = \pm\pi/2$; rotation is counter clockwise for $\alpha = \pi/2$, and the wave polarization is called left-circular; for $\alpha = -\pi/2$ we have clockwise rotation and right-circular polarization.

Polarization Ellipses

The ellipse traced by the electric field vector is illustrated in figure A-1 (note that positive θ and ϕ directions are downward and left, respectively).

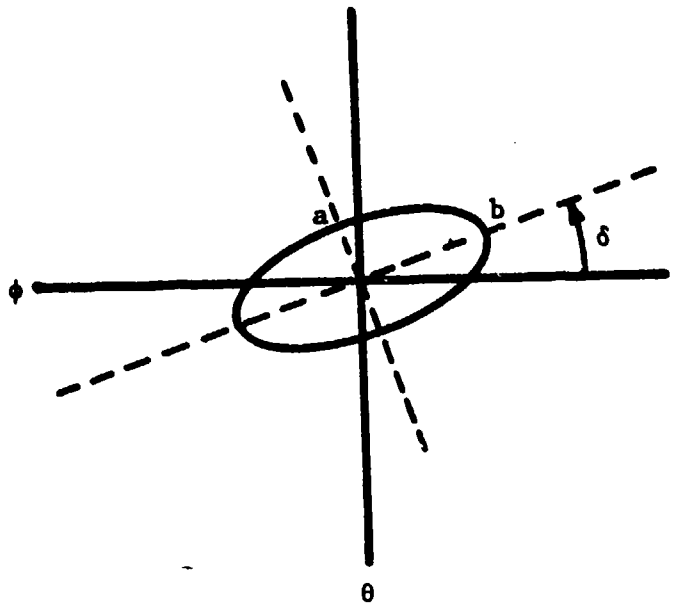

Figure A-1. Locus of tip of electric field vector for elliptical polarization.

Polarization can also be defined by the three quantities shown: a and b are ellipse minor and major axes half-lengths, respectively; δ is the tilt of the major axis from the ϕ axis. It can be shown that A, B, and α are related to a, b, and δ by

$$a^2 = \frac{2A^2B^2 \sin^2 \alpha}{(A^2 + B^2) - \sqrt{(A^2 + B^2)^2 - 4A^2B^2 \sin^2 \alpha}} \quad , \tag{A-3}$$

$$b^2 = \frac{2A^2B^2 \sin^2 \alpha}{(A^2 + B^2) + \sqrt{(A^2 + B^2)^2 - 4A^2B^2 \sin^2 \alpha}} \quad , \tag{A-4}$$

$$\tan 2\delta = \frac{2AB \cos \alpha}{B^2 - A^2} \quad . \tag{A-5}$$

The ratio a/b is often called <u>axial ratio</u> and is usually specified as a number greater than unity. Thus, if $a/b < 1$, axial ratio becomes b/a.

The reverse relationships are

$$A^2 = a^2 \sin^2 \delta + b^2 \cos^2 \delta \quad , \tag{A-6}$$

$$B^2 = a^2 \cos^2 \delta + b^2 \sin^2 \delta \quad , \tag{A-7}$$

$$\tan \alpha = \frac{2ab}{(a^2 - b^2) \sin 2\delta} \quad . \tag{A-8}$$

<u>Complex Fields and Wave Decomposition</u>

In the text fields are represented by complex quantities. The complex field components are the exponential extensions of equations (A-1) and (A-1); that is, E_θ is represented as the complex quantity, $A \exp(j\omega t)$. Usually, the common factor, $\exp(j\omega t)$, is suppressed since this carries through all steps in analysis. The remaining factor is called the complex envelope of the field. With these points in mind, fields in the text are complex with components

$$E_\theta = A \quad , \tag{A-9}$$

$$E_\phi = B\, e^{j\alpha} \quad . \tag{A-10}$$

In vector (matrix) notation these components give

$$\begin{bmatrix} E_\theta \\ E_\phi \end{bmatrix} = \begin{bmatrix} A \\ AQ \end{bmatrix} = A \begin{bmatrix} 1 \\ Q \end{bmatrix} \quad , \tag{A-11}$$

where we define a field component ratio,† denoted by Q, as

$$Q \triangleq E_\phi / E_\theta = B\, e^{j\alpha}/A \quad . \tag{A-12}$$

Table A-1 illustrates values of Q for some typical wave polarizations.

TABLE A-1. VALUES OF Q FOR VARIOUS WAVE POLARIZATIONS.

Wave Polarization	Q	A	B	α
Linear in θ direction	0	arbitrary $\neq 0$	0	0
Linear in ϕ direction	∞	0	arbitrary $\neq 0$	0
Linear tilted by angle ϕ_0 from ϕ axis	$\cot \phi_0$	arbitrary	$A \cot \phi_0$	0
Left circular	j	arbitrary	$= A$	$\pi/2$
Right circular	-j	arbitrary	$= A$	$-\pi/2$

If equation (A-11) represents electric field vector $\vec{E}$, the magnitude squared of $\vec{E}$ is

$$|\vec{E}|^2 = \begin{bmatrix} E_\theta^* & E_\phi^* \end{bmatrix} \begin{bmatrix} E_\theta \\ E_\phi \end{bmatrix} = |E_\theta|^2 + |E_\phi|^2 = |A|^2[1 + |Q|^2] \quad . \tag{A-13}$$

Next, let $\vec{E}$ represent an arbitrarily polarized field given by equation (A-11) and let two other elliptically polarized waves be described by

---

†This ratio has also been called a "polarization factor" by Beckmann and Spizzichino [37] and given a symbol different than Q.

$$\vec{E}_1 = \begin{bmatrix} A_1 \\ A_1 Q_1 \end{bmatrix}, \quad \vec{E}_2 = \begin{bmatrix} A_3 \\ A_2 \end{bmatrix} . \tag{A-14}$$

We show that $\vec{E}$ can be decomposed into the sum of $\vec{E}_1$, having an arbitrary (selected) elliptical polarization set by Q_1, and $\vec{E}_2$, which has the elliptical polarization orthogonal to that of $\vec{E}_1$. Since $\vec{E}_1$ and $\vec{E}_2$ are to be orthogonal their inner product is zero, and

$$\vec{E}_1 \cdot \vec{E}_2 = \begin{bmatrix} A_1^* & A_1^* Q_1^* \end{bmatrix} \begin{bmatrix} A_3 \\ A_2 \end{bmatrix} = A_1^* A_3 + A_1^* Q_1^* A_2 = 0 \quad , \tag{A-15}$$

which requires $A_3 = -A_2 Q_1^*$ for any A_2. Thus, we require

$$\vec{E} = \begin{bmatrix} A \\ AQ \end{bmatrix} = \vec{E}_1 + \vec{E}_2 = \begin{bmatrix} A_1 \\ A_1 Q_1 \end{bmatrix} + \begin{bmatrix} -A_2 Q_1^* \\ A_2 \end{bmatrix} = \begin{bmatrix} A_1 - A_2 Q_1^* \\ A_1 Q_1 + A_2 \end{bmatrix}$$
$$= \begin{bmatrix} 1 & -Q_1^* \\ Q_1 & 1 \end{bmatrix} \begin{bmatrix} A_1 \\ A_2 \end{bmatrix} . \tag{A-16}$$

After solving equation (A-16) for A_1 and A_2, we have

$$A_1 = \frac{A(1 + QQ_1^*)}{1 + |Q_1|^2} \quad , \tag{A-17}$$

$$A_2 = \frac{A(Q - Q_1)}{1 + |Q_1|^2} \quad . \tag{A-18}$$

These results show that any elliptically polarized wave can be decomposed into the sum of one elliptically polarized field of specified polarization and "amplitude" given by equation (A-17) and another wave with "amplitude" given by equation (A-18) with polarization orthogonal to the specified wave. This means any received wave can be separated into the component to which a given antenna responds plus another component to which it does not respond.

Finally, we note that the powers in the two received waves are proportional to $|\hat{E}_1|^2$ and $|\hat{E}_2|^2$

$$|\hat{E}_1|^2 = |A_1|^2(1 + |Q_1|^2) \quad , \tag{A-19}$$

$$|\hat{E}_2|^2 = |A_2|^2(1 + |Q_1|^2) \quad . \tag{A-20}$$

DISTRIBUTION

	Copies
Administrator **Defense Technical Information Center**	
ATTN: DTIC-DCA	12
Cameron Station, Building 5 **Alexandria, VA 22314**	
US Army Electronics Research & Development Command	
ATTN: Commander, DRDEL-CG	1
ATTN: Technical Director, DRDEL-CT	1
ATTN: Public Affairs Office, DRDEL-IN	1
2800 Powder Mill Road **Adelphi, MD 20783**	
Harry Diamond Laboratories	
ATTN: CO/TD/TSO/Division Directors	1
ATTN: Record Copy, 81200	1
ATTN: HDL Library, 81100	3
ATTN: HDL Library, 81100 (Woodbridge)	1
ATTN: Technical Reports Branch, 81300	1
ATTN: Chairman, Editorial Committee	1
ATTN: Legal Office, 97000	1
ATTN: Chief, Branch 11400	10
2800 Powder Mill Road **Adelphi, MD 20783**	